Available online at www.sciencedirect.com
ScienceDirect
Journal of Power Sources 159 (2006) 690–701
JOURNAL OF POWER SOURCES
www.elsevier.com/locate/jpowsour

# Conductivity studies on ceramic $Li_{1.3}Al_{0.3}Ti_{1.7}(PO_4)_3$-filled PEO-based solid composite polymer electrolytes

Yan-Jie Wang [a,b], Yi Pan [a], Dukjoon Kim [b,*]

[a] *Department of Materials Science and Engineering, Zhejiang University, Hangzhou, 310027, PR China*
[b] *Department of Chemical Engineering, Polymer Technology Institute, Sungkyunkwan University, Suwon, Kyunggi, 440-746, South Korea*

Received 11 July 2005; accepted 29 October 2005
Available online 13 December 2005

**Abstract**

With the promise of its high conductivity, the ceramic $Li_{1.3}Al_{0.3}Ti_{1.7}(PO_4)_3$ ($x = 0.85$) of $Li_{3-2x}(Al_{1-x}Ti_x)_2(PO_4)_3$ ($x = 0.55$ to 1.0), as a lithium fast ionic conductor, is produced by a conventional solid-state reaction and introduced into the poly(ethylene oxide) (PEO)-based composite polymer electrolyte films (CPE) to improve their ionic conductivity. The CPE films are prepared by a solution-cast technique and their characteristics are investigated by several experimental techniques including X-ray diffraction (XRD), infrared (IR) spectra, differential scanning calorimetry (DSC), and scanning electron microscopy (SEM). As measured by electrochemical impedance spectrum (EIS) measurement, the temperature-dependent ionic conductivity of PEO–$Li_{1.3}Al_{0.3}Ti_{1.7}(PO_4)_3$ film with EO/Li = 16 is maximized at $2.631 \times 10^{-6}$ S cm$^{-1}$ at room temperature and at $1.185 \times 10^{-4}$ S cm$^{-1}$ at 343 K, while the ionic conductivity of the PEO–$LiClO_4$–$Li_{1.3}Al_{0.3}Ti_{1.7}(PO_4)_3$ film with EO/Li = 8 is maximized at $7.985 \times 10^{-6}$ S cm$^{-1}$ at room temperature and at $1.161 \times 10^{-3}$ S cm$^{-1}$ at 373 K when $Li_{1.3}Al_{0.3}Ti_{1.7}(PO_4)_3$ content is 15 wt.%.


*Keywords:* Poly(ethylene oxide); Composite polymer electrolyte; Ionic conductivity; Lithium rechargeable batteries; Temperature dependence

## 1. Introduction

After the report by Wright [1] on ion conduction in a poly(ethylene oxide) (PEO)–alkali metal salt complex, and the suggestion by Armand et al. [2,3] that an ion conducting polymer could be used as a solid electrolyte in a battery of high specific energy, research on ion-conducting solid polymer electrolytes (SPEs) has attracted world-wide attention because of the product's high potential for use in lithium rechargeable batteries, fuel cells, electrochemical sensors, and other electrochemical devices. PEO as a matrix in the ion-conducting SPE can be seen as a solid solution of alkali metal salts in the polymer that dissociates into free ions under the coordinating effects of neighboring polymer segments containing polar groups that consist of oxygen atoms. The segments can rearrange their position and configuration, and thus change the location of ions. The local relaxation and segmental motion of the polymer chains are important for the transport of lithium ions in PEO. It is also widely accepted that the ionic conductivity is attributed to the amorphous, rather than crystalline, regions in a PEO–LiX complex [4]. This condition can only be obtained when the polymer is in an amorphous state.

The main drawback of solvent-free, PEO-based, polymer electrolytes is their crystalline state at room temperature. This reduces the conductivity to a level that is too low to satisfy the general requirements of batteries or of other practical electrochemical devices. Therefore, to improve the ion conductivity at ambient temperature, research has continued for several years into the addition of inorganic fillers such as $Al_2O_3$, $TiO_2$, $SiO_2$ and $Sm_2O_3$ to a PEO–LiX SPE [5–9]. None of these inorganic powders is an ionic conductor that offers lithium ions in polymer electrolytes, whereas the ceramic $Li_{3-2x}(Al_{1-x}Ti_x)_2(PO_4)_3$ ($x = 0.55$–1.0) is a lithium fast ionic conductor that is produced by a conventional solid-state reaction [10]. It has a high conductivity (>$10^{-6}$ S cm$^{-1}$) and high ion transport number ($t_1 \approx 1$). To facilitate the ionic conductivity, $Li_{1.3}Al_{0.3}Ti_{1.7}(PO_4)_3$ ($x = 0.85$) powders have been introduced into a PEO-based polymer electrolyte. The compound $Li_{3-2x}(Al_{1-x}Ti_x)_2(PO_4)_3$, has been derived from the lithium fast ionic conductors $Li_{3-2x}(Sc_{1-x}Ti_x)_2(PO_4)_3$, where Sc is

* Corresponding author. Tel.: +82312907250; fax: +82312907272.
*E-mail address:* djkim@skku.edu (D. Kim).

0378-7753/$ – see front matter © 2005 Elsevier B.V. All rights reserved.
doi:10.1016/j.jpowsour.2005.10.104

replaced by Al. $LiSc_2(PO_4)_3$ has been reported [11] as a lithium ionic conductor with good ionic conductivity at ambient temperature. Its γ-phase has three lithium sites per formula that are partially occupied in a similar manner to Nasicon-type $LiM_2(PO_4)_3$ (M = Ti, Ge, Zr, Hf) [12–14]. Through the substitution of Ti for part of the Sc in $LiSc_2(PO_4)_3$, $Li_{3-2x}(Sc_{1-x}Ti_x)_2(PO_4)_3$ has been produced with an ionic conductivity is higher than that of $LiSc_2(PO_4)_3$ [15]. Based on this ionic conductivity advantage of $Li_{3-2x}(Sc_{1-x}Ti_x)_2(PO_4)_3$ and on the conductivity improvement gained since the Al atom is smaller than Sc and since they are all trivalent elements, $Li_{3-2x}(Al_{1-x}Ti_x)_2(PO_4)_3$ ($x = 0.55$–1.0), which can also be considered to result from the part replacement of Ti to Al in $LiTi_2(PO_4)_3$, warrants synthesis and study to find the optimum compound with the best ionic conductivity for application in PEO-based solid composite polymer electrolytes (CPEs).

In the present study, $Li_{3-2x}(Al_{1-x}Ti_x)_2(PO_4)_3$ ($x = 0.55$–1.0) was synthesized and $Li_{1.3}Al_{0.3}Ti_{1.7}(PO_4)_3$ ($x = 0.85$), which demonstrated the best ionic conductivity, underwent study by XRD and temperature-dependent conductivity measurement. Meanwhile, PEO-based solid CPE films with different $Li_{1.3}Al_{0.3}Ti_{1.7}(PO_4)_3$ ($x = 0.85$) content were prepared by a solution-cast technique. In addition to several experimental techniques, including X-ray diffraction (XRD), infrared (IR) spectra, differential scanning calorimetry (DSC) and scanning electron microscopy (SEM), that were employed to characterize these polymeric electrolyte films, electrochemical impedance spectrum (EIS) measurement was used to study the ionic conductivity as a function of temperature for these materials. The results are reported and discussed in terms of the relationships between the ionic conductivity and the structure of $Li_{1.3}Al_{0.3}Ti_{1.7}(PO_4)_3$-filled, PEO-based, solid CPE films.

## 2. Experimental

### 2.1. Materials and sample preparation

Starting from the reagent grade chemicals of $Li_3PO_4$, $Al_2O_3$, $TiO_2$ and $NH_4H_2PO_4$, the $Li_{3-2x}(Al_{1-x}Ti_x)_2(PO_4)_3$ system ($x = 0.55, \ldots, 1.0$) was prepared using a conventional solid-state reaction as described by Suzuki et al. [10]. In terms of ionic conductivity measurements on these phosphates, the compound $Li_{1.3}Al_{0.3}Ti_{1.7}(PO_4)_3$ ($x = 0.85$) had the highest ionic conductivity and was chosen as the lithium-ion conductive constituent in the polymer electrolyte after ball-milling for 72 h. The fine particles of ball-milled $Li_{1.3}Al_{0.3}Ti_{1.7}(PO_4)_3$, the particle distribution of which is illustrated in Fig. 1 and which was thought to be satisfactory for this study, were dried under vacuum at 120 °C for 48 h to remove all possibly attached water molecules. Lithium perchlorate ($LiClO_4$) obtained from Zhangjiagang Guotai-Huarong New Chemical Materials Co. Ltd. in China was dried under vacuum at 120 °C for 24 h to remove water before being used. The PEO polymer in powder form (Aldrich, $M_n = 1{,}000{,}000$) was purchased from Aldrich Chem. Co. and dried under vacuum at 50 °C for 48 h for the use as the CPE matrix. Acetonitrile, which served as the intermediate medium for the material, was doubly distilled and stored over a 4 Å molecular sieves.

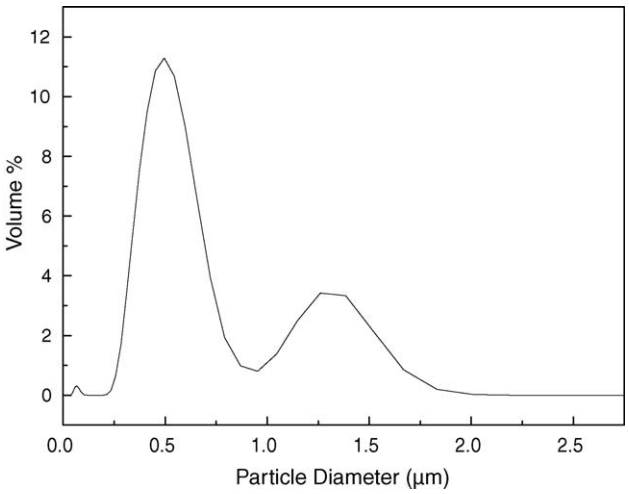


Fig. 1. Particle size distribution of $Li_{1.3}Al_{0.3}Ti_{1.7}(PO_4)_3$ salts after ball milling.

Two PEO-based CPE films, i.e. PEO–$Li_{1.3}Al_{0.3}Ti_{1.7}(PO_4)_3$ system with various EO/Li molar ratios and PEO–$LiClO_4$–$Li_{1.3}Al_{0.3}Ti_{1.7}(PO_4)_3$ system with EO/Li = 8 (Li from $LiClO_4$ and $Li_{1.3}Al_{0.3}Ti_{1.7}(PO_4)_3$) and different $Li_{1.3}Al_{0.3}Ti_{1.7}(PO_4)_3$ contents, were prepared in a dry atmosphere by magnetically stirring weighted quantities of 4–5% acetonitrile solutions of each component in the temperature range of 60–70 °C for 24 h. The electrolyte films were cast on to a finely-polished Teflon support. After slow evaporation of the solvent at room temperature, the solid membranes (150–300 μm thick) were dried under a high vacuum for 24 h at 50 °C and sealed in a glass desiccator in a dry room until use.

### 2.2. Measurements

The phase analyses were conducted for $Li_{3-2x}(Al_{1-x}Ti_x)_2(PO_4)_3$ ($x = 0.55$–1.0) and two PEO-based CPE films using an X-ray diffractometer (Bruker-AXS) with Cu Kα radiation and a step-scanning method with a step width of 0.02° at room temperature (~25 °C). The equipment was operated at 30 kV. DSC data were obtained between −100 and 100 °C by means of a model Q100 V7.3 instrument (TA Company, USA) with a low-temperature measurement, liquid nitrogen-cooled heating element. The samples to be analyzed were sealed in aluminum pans. Each sample was first heated from 25 to 100 °C at a heating rate of 10 °C $min^{-1}$. After thermal stabilization, the chosen sample was cooled to −100 °C at the same rate, using liquid nitrogen, and then heated at 10 °C $min^{-1}$ to 100 °C. All IR absorption spectra were taken on a Perkin-Elmer FTIR spectrometer (model 1605) over the range 4000 to 450 $cm^{-1}$. The SEM studies were conducted on a Hitachi S-570 scanning electron microscope. Thin electrolyte films prepared by a solution-cast technique were mounted on 1 cm diameter aluminum plates. Samples were sputter-graphite-coated (20 nm). The surface morphology of all specimens was examined at a working voltage of 25 kV. Ionic conductivity was determined using an EIS method over a range of temperatures. $Li_{3-2x}(Al_{1-x}Ti_x)_2(PO_4)_3$ specimens were

coated with silver paste and then heated to solidify the paste to form the electrodes for ionic conductivity measurements. Samples of the polymer electrolyte film were sandwiched between stainless-steel blocking electrodes and placed in a temperature-controlled furnace. The impedance measurements were carried out with a frequency response analyzer (FRA Solartron model 1255) and a Solartron model 1287 electrochemical interface over the frequency range 0.01 Hz to 1 MHz.

## 3. Results and discussion

### 3.1. XRD studies

The XRD patterns for the $Li_{3-2x}(Al_{1-x}Ti_x)_2(PO_4)_3$ system are given in Fig. 2. It is obvious that $LiTi_2(PO_4)_3$ is the major crystalline phase in all the inorganic specimens. Some unknown phases begin to appear at $x = 0.65$ then grow thereafter. This suggests that the substitution of $Al^{3+}$ ions for $Ti^{4+}$ takes place in the Nasicon-type $LiTi_2(PO_4)_3$. For $Li_{3-2x}(Al_{1-x}Ti_x)_2(PO_4)_3$ from $x = 1.0$–$0.70$, since no obvious new peak appears as $Al^{3+}$ ions replace $Ti^{4+}$ ions, it is inferred that the added $Al^{3+}$ ions are incorporated into the structure of $LiTi_2(PO_4)_3$ by replacing the $Ti^{4+}$ ions. A slight shift in the position of the diffraction peak towards a higher diffraction angle until $x = 0.55$ is observed for $LiTi_2(PO_4)_3$, which confirms that the replacement occurs because of the smaller ionic radius of $Al^{3+}$ (0.535 Å) compared with that of $Ti^{4+}$ (0.605 Å). Therefore, it is concluded that $LiTi_2(PO_4)_3$ is the major crystalline phase for $Li_{1.3}Al_{0.3}Ti_{1.7}(PO_4)_3$ ($x = 0.85$), and that $Al^{3+}$ ions replace $Ti^{4+}$ ions and are incorporated into the structure of $LiTi_2(PO_4)_3$.

The X-ray traces performed at room temperature for two PEO-based CPE films are given in Fig. 3(Panel A), EO/Li = 0 corresponds to $Li_{1.3}Al_{0.3}Ti_{1.7}(PO_4)_3$ and EO/Li = infinity corresponds to pure PEO. It is clear that there are two strong peaks at $2\theta = 19.5^\circ$ and $23.5^\circ$ and this demonstrates a high degree of crystallization in pure PEO. The partial crystallization of the polymer results from the high inherent crystallinity of PEO in the absence of the $Li_{1.3}Al_{0.3}Ti_{1.7}(PO_4)_3$ salt. The two peaks decrease as more lithium salt is added. The crystalline area into which no lithium salt is incorporated may have been squeezed by the highly $Li_{1.3}Al_{0.3}Ti_{1.7}(PO_4)_3$ loaded amorphous areas, which thereby reduces the crystalline plane spacing of the PEO matrix. The crystal structure of the lithium salt added to the PEO matrix does not change much, but the peaks broadened with decreasing salt content. Broadening of the peaks is attributed to a reduction in particle size with decreasing salt content, which indicates the partial dissolution of the salt in the amorphous regions of the PEO matrix. Thus, the X-ray traces suggest that there may be two regions in PEO–$Li_{1.3}Al_{0.3}Ti_{1.7}(PO_4)_3$ salt films, namely, uncomplexed (mixture of crystalline PEO and $Li_{1.3}Al_{0.3}Ti_{1.7}(PO_4)_3$) and complexed (amorphous with $Li_{1.3}Al_{0.3}Ti_{1.7}(PO_4)_3$) PEO.

An interesting feature in Fig. 3(B) is the decreasing intensity of the two strong peaks at $2\theta = 19.5^\circ$ and $23.5^\circ$ in pure PEO with decreasing $Li_{1.3}Al_{0.3}Ti_{1.7}(PO_4)_3$ content in the PEO–$LiClO_4$–$Li_{1.3}Al_{0.3}Ti_{1.7}(PO_4)_3$ films, although the $LiClO_4$ content relatively increases with decreasing

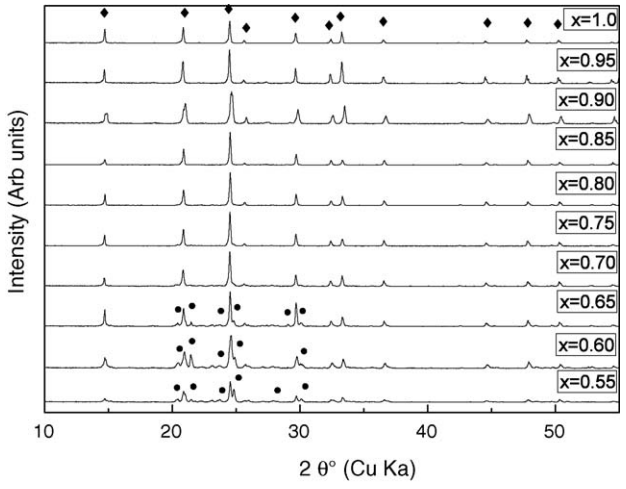


Fig. 2. X-ray diffraction patterns of $Li_{3-2x}(Al_{1-x}Ti_x)_2(PO_4)_3$ system ($x = 0.5$, 0.55, …, 1.0). The most characteristic peaks for some crystalline phases are indicated: (♦) $LiTi_2(PO_4)_3$; (●) new unknown phase.

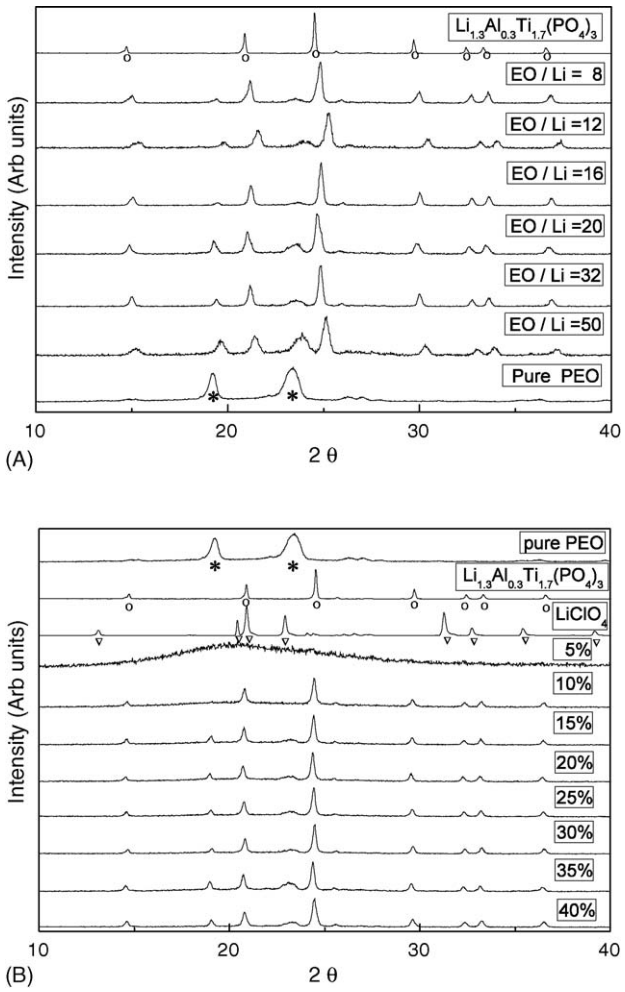


Fig. 3. (A) X-ray diffraction patterns of selected PEO–$Li_{1.3}Al_{0.3}Ti_{1.7}(PO_4)_3$ films at room temperature. The monomer unit EO/Li molar ratio is indicated on each spectrum. The most characteristic peaks for some crystalline phases are indicated: (*) PEO; (◯) $Li_{1.3}Al_{0.3}Ti_{1.7}(PO_4)_3$ salt. (B) X-ray diffraction patterns of selected PEO–$LiClO_4$–$Li_{1.3}Al_{0.3}Ti_{1.7}(PO_4)_3$ films at room temperature.

$Li_{1.3}Al_{0.3}Ti_{1.7}(PO_4)_3$ content. For $Li_{1.3}Al_{0.3}Ti_{1.7}(PO_4)_3$ contents from 10 to 40 wt.%, some characteristic peaks of $Li_{1.3}Al_{0.3}Ti_{1.7}(PO_4)_3$ salt appear and their widths slightly increases, despite the fact that: these are no visible characteristic peaks of $LiClO_4$, even at the maximum $LiClO_4$ content of 5 wt.% of $Li_{1.3}Al_{0.3}Ti_{1.7}(PO_4)_3$ content. It is inferred that a complexation between $LiClO_4$ and PEO must have occurred and that the $Li_{1.3}Al_{0.3}Ti_{1.7}(PO_4)_3$ salt is partly dissolved in the amorphous regions of the PEO matrix. Nevertheless, the crystalline area in the PEO–$LiClO_4$–$Li_{1.3}Al_{0.3}Ti_{1.7}(PO_4)_3$ films may still have been squeezed by the $Li_{1.3}Al_{0.3}Ti_{1.7}(PO_4)_3$ loaded amorphous areas.

Therefore, in $Li_{1.3}Al_{0.3}Ti_{1.7}(PO_4)_3$-filled, PEO-based CPEs, $Li_{1.3}Al_{0.3}Ti_{1.7}(PO_4)_3$ severely effects the crystallization of the PEO matrix. When $LiClO_4$ and $Li_{1.3}Al_{0.3}Ti_{1.7}(PO_4)_3$ are both added to PEO, the results suggest that the decrease of crystallization of the polymer electrolyte can be attributed to the complexation between PEO and $LiClO_4$ in PEO-based CPEs rather than to that between PEO and $Li_{1.3}Al_{0.3}Ti_{1.7}(PO_4)_3$.

### 3.2. DSC studies

The DSC thermograms obtained in the second heating scan for PEO–$Li_{1.3}Al_{0.3}Ti_{1.7}(PO_4)_3$ and PEO–$LiClO_4$–$Li_{1.3}Al_{0.3}Ti_{1.7}(PO_4)_3$ materials are displayed in Fig. 4(A) and (B), respectively. It is clear that no heat flow is detected in the DSC thermograms up to 70 °C for pure $Li_{1.3}Al_{0.3}Ti_{1.7}(PO_4)_3$. Exothermic peaks are seen for PEO–$Li_{1.3}Al_{0.3}Ti_{1.7}(PO_4)_3$ materials with different EO/Li molar ratios in the materials. The temperature at which the peak occurs is the crystallization temperature ($T_c$) of each material and equals the melting temperature ($T_m$), i.e. the PEO matrix in this study. With the addition of $Li_{1.3}Al_{0.3}Ti_{1.7}(PO_4)_3$ and a decrease in the EO/Li molar ratio, the exothermic peak broadens and shifts towards low $T_c$, see Fig. 4(A). The crystalline part of the PEO matrix in the PEO–$Li_{1.3}Al_{0.3}Ti_{1.7}(PO_4)_3$ system is squeezed or strained, as evidenced by the right shift of the PEO diffraction peaks as the EO/Li molar ratio is decreased (see Fig. 3, panel A). The squeezed or strained PEO melts at a relatively low temperature because of the strain energy. The DSC curves for PEO–$LiClO_4$–$Li_{1.3}Al_{0.3}Ti_{1.7}(PO_4)_3$ films with various amounts of $Li_{1.3}Al_{0.3}Ti_{1.7}(PO_4)_3$ salt and EO/Li = 8 are displayed in Fig. 4(B). This is a distinctive exothermic peak that corresponds to the melting of the crystalline phase. The glass transition temperature ($T_g$), $T_m$, $\Delta H_{m,CPE}$ and degree of crystallinity ($\chi_c$) are summarized in Table 1 for all the films. In all films, $\chi_c$ increases from 4.36 to 28.53% (which is still much lower than the degree of crystallinity (50.34%) of pure PEO below its melting point) with the increase in $Li_{1.3}Al_{0.3}Ti_{1.7}(PO_4)_3$ salt content from 5 to 40 wt.%. Chu et al. [7] reported that $Sm_2O_3$ addition led to the PEO–$LiClO_4$ system being less crystalline and that 20 wt.% $Sm_2O_3$ lowered the crystallinity from 49.7 to 37% [7]. In terms of a decrease in crystallinity, $Li_{1.3}Al_{0.3}Ti_{1.7}(PO_4)_3$ addition is more effective than $Sm_2O_3$ addition, probably because $Li_{1.3}Al_{0.3}Ti_{1.7}(PO_4)_3$ is also an ionic conductor and is therefore able to dissolve in, or complex with, the PEO to some extent. In addition, $T_m$ increases from 28.85 to 53.79 °C, which nevertheless remains less than the melting point of pure PEO (63.67 °C), with increasing $Li_{1.3}Al_{0.3}Ti_{1.7}(PO_4)_3$ content from 5 to 40 wt.%. This result is also different from the situation involving $Sm_2O_3$ in the PEO–$LiClO_4$ system. With increasing $Sm_2O_3$ addition, the melting point decreases, but the maximum reduction is much less than that of $Li_{1.3}Al_{0.3}Ti_{1.7}(PO_4)_3$. The trend for $T_g$ means in a opposite direction to that of $T_m$, i.e. $T_g$ decreases with

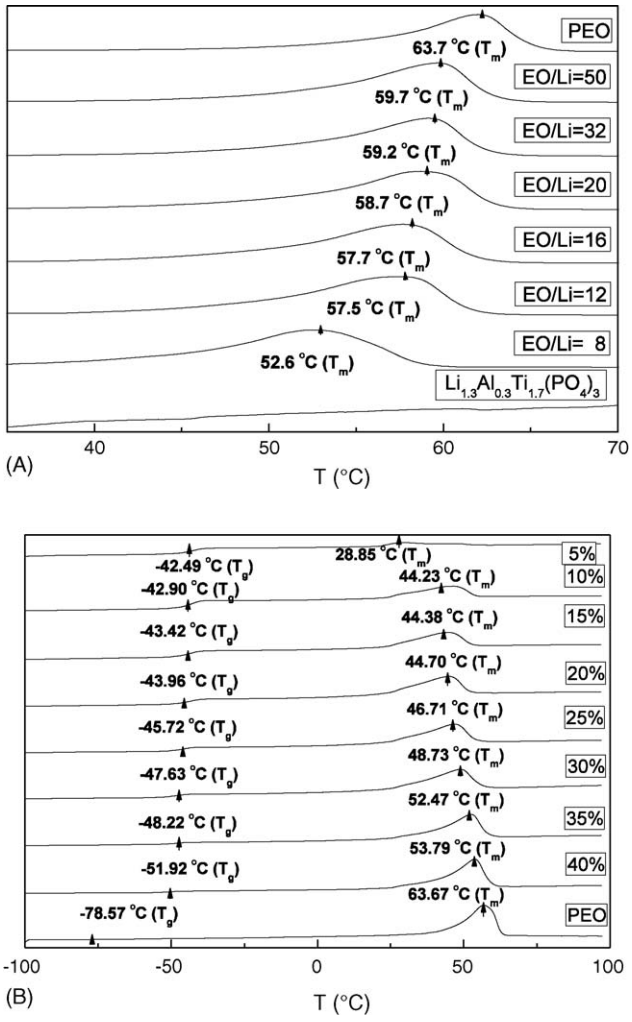


Fig. 4. (A) DSC curves of selected PEO–$Li_{1.3}Al_{0.3}Ti_{1.7}(PO_4)_3$ materials. (B) DSC traces of PEO–$LiClO_4$–$Li_{1.3}Al_{0.3}Ti_{1.7}(PO_4)_3$ for different contents of $Li_{1.3}Al_{0.3}Ti_{1.7}(PO_4)_3$.

Table 1
Thermal properties of PEO–$LiClO_4$–$Li_{1.3}Al_{0.3}Ti_{1.7}(PO_4)_3$ samples

| $Li_{1.3}Al_{0.3}Ti_{1.7}(PO_4)_3$ content (wt.%) | $T_g$ (°C) | $T_m$ (°C) | $\Delta H_m$ (J/g) | $\chi_e$ (%) |
|---|---|---|---|---|
| Pure PEO | −78.57 | 63.67 | 94.64 | 50.34 |
| 5 | −42.49 | 28.85 | 8.189 | 4.36 |
| 10 | −42.90 | 44.23 | 16.20 | 8.62 |
| 15 | −43.42 | 44.38 | 21.34 | 11.35 |
| 20 | −43.96 | 44.70 | 29.05 | 15.45 |
| 25 | −45.72 | 46.71 | 32.81 | 17.45 |
| 30 | −47.63 | 48.73 | 34.74 | 18.48 |
| 35 | −48.22 | 52.47 | 47.70 | 25.37 |
| 40 | −51.92 | 53.79 | 53.64 | 28.53 |

increasing $Li_{1.3}Al_{0.3}Ti_{1.7}(PO_4)_3$ content. As suggested above, the addition of $LiClO_4$ in PEO lowers the crystallinity of PEO. The substitution of $Li_{1.3}Al_{0.3}Ti_{1.7}(PO_4)_3$ for $LiClO_4$ by maintaining EO/Li = 8 retrieves the crystallinity (although it remains very effective in reducing the crystallinity) and yet raises the flexibiltiy of the EO chains.

Therefore, in the study of the CPE structural changes through heat treatment, DSC thermograms (see Fig. 4) indicate that $T_m$ decreases and PEO crystallinity deteriorates an the addition of $Li_{1.3}Al_{0.3}Ti_{1.7}(PO_4)_3$ salt. These results are beneficial for the production of highly-conductive CPEs because increase in the amorphous extent of PEO with concomitant decrease in crystallinity can improve the ionic conductivity [16].

### 3.3. FT-IR spectroscopy

The complexation of PEO with some salts has also been studied by means of IR spectra measurements [17,18]. The results for PEO–$Li_{1.3}Al_{0.3}Ti_{1.7}(PO_4)_3$ and PEO–$LiClO_4$–$Li_{1.3}Al_{0.3}Ti_{1.7}(PO_4)_3$ are shown in Fig. 5.

The spectra of PEO–$Li_{1.3}Al_{0.3}Ti_{1.7}(PO_4)_3$ films show differences from those of pure PEO and $Li_{1.3}Al_{0.3}Ti_{1.7}(PO_4)_3$. The peaks at about 2900 and 1100 $cm^{-1}$ in pure PEO are believed to be from the vibrations of C–H and C–O bonds, respectively. After the addition of $Li_{1.3}Al_{0.3}Ti_{1.7}(PO_4)_3$, the width and intensity of peak at about 2900 $cm^{-1}$ decreases with decreasing EO/Li molar ratio, while the existing peak at 1100 $cm^{-1}$ and another peak at 3445.5 $cm^{-1}$ in pure PEO are incorporated by the peaks at 1028.3 $cm^{-1}$ and 3441.7 $cm^{-1}$ from pure $Li_{1.3}Al_{0.3}Ti_{1.7}(PO_4)_3$ salt, respectively. Both these peaks are shifted to the right with decrease in the EO/Li molar ratio. With increasing EO/Li molar ratio in the film, the peaks at 570.82, 640.25, 1028.3, 1224.58, 1642.9, 2856.06, 2924.9 and 3441.7 $cm^{-1}$ originally found in the IR spectra of pure $Li_{1.3}Al_{0.3}Ti_{1.7}(PO_4)_3$ are slightly shifted to left and become narrower. Moreover, peaks at 529.0, 842.3, 959.3, 1241.9, 1282.1, 1344.8 and 1468.2 belonging to pure PEO merged in the PEO–$Li_{1.3}Al_{0.3}Ti_{1.7}(PO4)_3$ films, even at high PEO concentration. In addition, in each of those films with EO/Li molar ratios of 8, 12 and 16, a new peak around at 2368 $cm^{-1}$ is observed.

The above changes with changing EO/Li ratio of the PEO–$Li_{1.3}Al_{0.3}Ti_{1.7}(PO_4)_3$ films suggests that some bonds in PEO are influenced by the addition of $Li_{1.3}Al_{0.3}Ti_{1.7}(PO_4)_3$ to pure PEO. The new peak at around 2368 $cm^{-1}$ and the changes

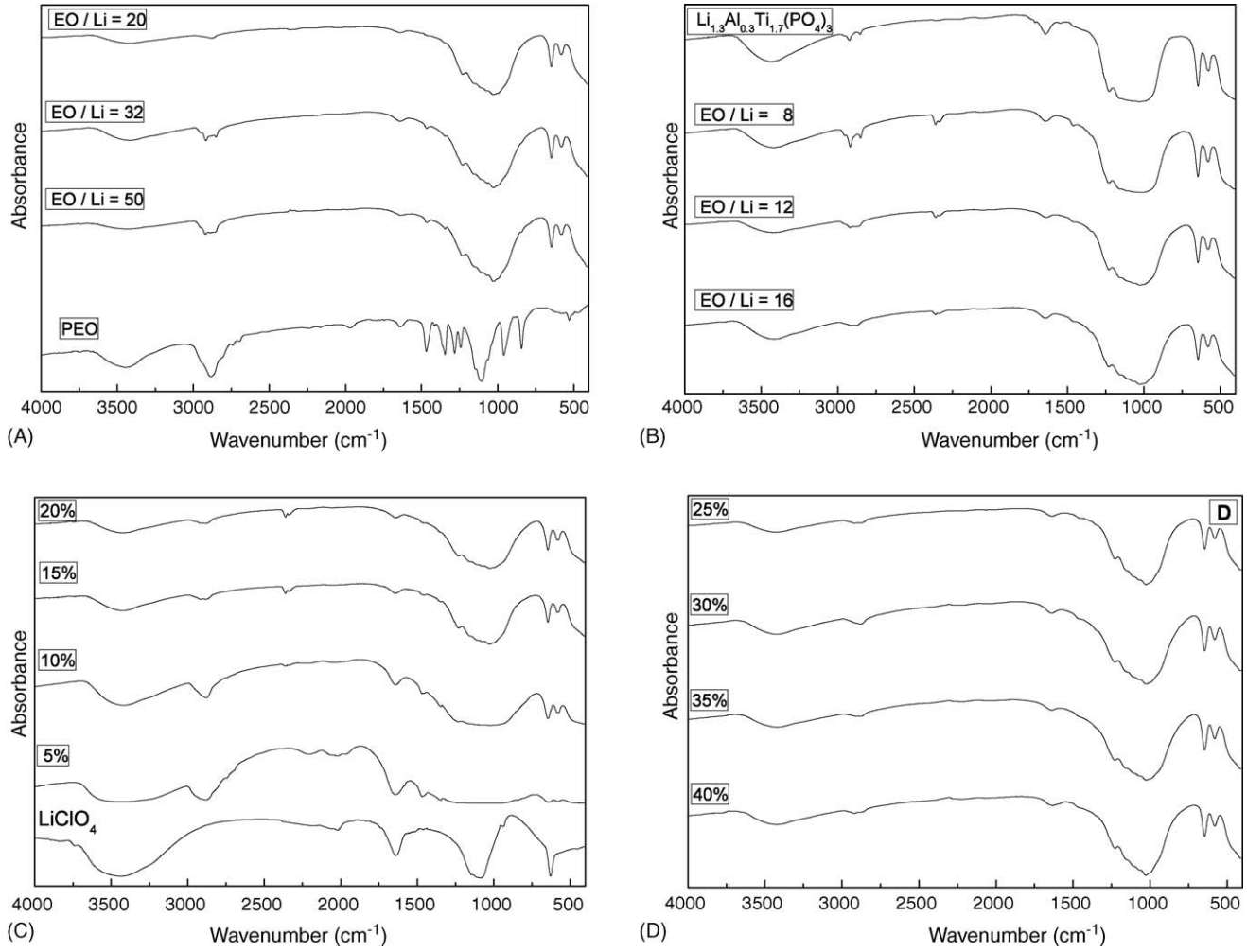


Fig. 5. (A, B) Infrared spectra of selected PEO–$Li_{1.3}Al_{0.3}Ti_{1.7}(PO_4)_3$ films. (C, D) Infrared spectra of selected PEO–$LiClO_4$–$Li_{1.3}Al_{0.3}Ti_{1.7}(PO_4)_3$ films.

of the original peaks belonging to the two components demonstrated the ability of PEO to complex with $Li_{1.3}Al_{0.3}Ti_{1.7}(PO_4)_3$ to some extent, and that this complexation only depends on the EO/Li molar ratio, i.e. on the $Li_{1.3}Al_{0.3}Ti_{1.7}(PO_4)_3$ content in PEO.

The IR spectra of the PEO–$LiClO_4$–$Li_{1.3}Al_{0.3}Ti_{1.7}(PO_4)_3$ films, given in Fig. 5(C) and (D), show that as the $Li_{1.3}Al_{0.3}Ti_{1.7}(PO_4)_3$ content decreases, the intensity of some peaks at 570.82, 640.25, 1028.3 and 1224.58 $cm^{-1}$, which are originally found in the IR spectra of $Li_{1.3}Al_{0.3}Ti_{1.7}(PO_4)_3$,

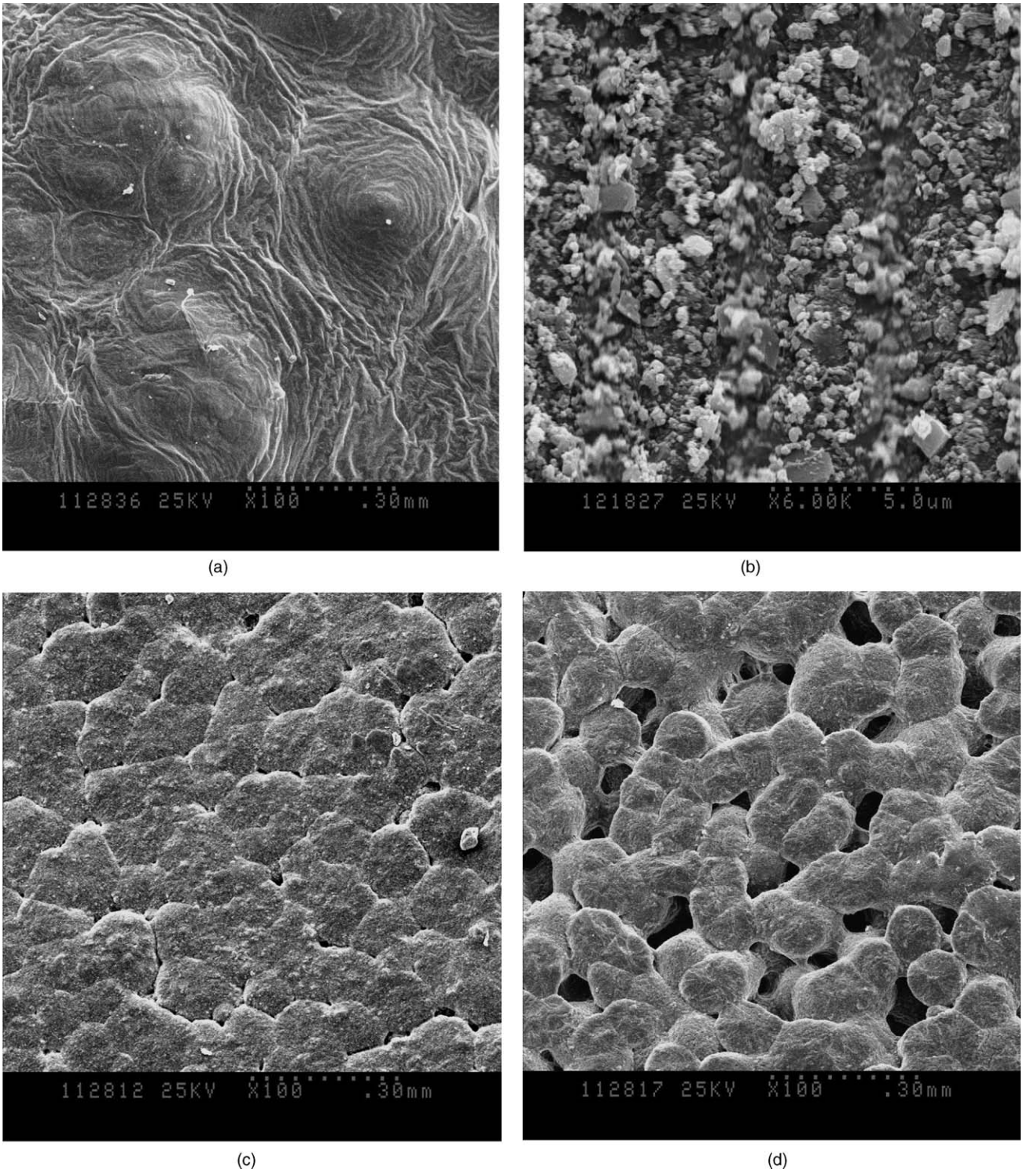


Fig. 6. Scanning electron micrographs of: (a) pure PEO; (b) fine $Li_{1.3}Al_{0.3}Ti_{1.7}(PO_4)_3$ powder; (c) EO/Li = 8; (d) EO/Li = 12; (e) EO/Li = 20; (f) EO/Li = 32; (g) 5 wt.% $Li_{1.3}Al_{0.3}Ti_{1.7}(PO_4)_3$; (h) 10 wt.% $Li_{1.3}Al_{0.3}Ti_{1.7}(PO_4)_3$; (i) 15 wt.% $Li_{1.3}Al_{0.3}Ti_{1.7}(PO_4)_3$; (j) 20 wt.% $Li_{1.3}Al_{0.3}Ti_{1.7}(PO_4)_3$; (k) 25 wt.% $Li_{1.3}Al_{0.3}Ti_{1.7}(PO_4)_3$; (l) 30 wt.% $Li_{1.3}Al_{0.3}Ti_{1.7}(PO_4)_3$; (m) 35 wt.% $Li_{1.3}Al_{0.3}Ti_{1.7}(PO_4)_3$; and (n) 40 wt.% $Li_{1.3}Al_{0.3}Ti_{1.7}(PO_4)_3$.

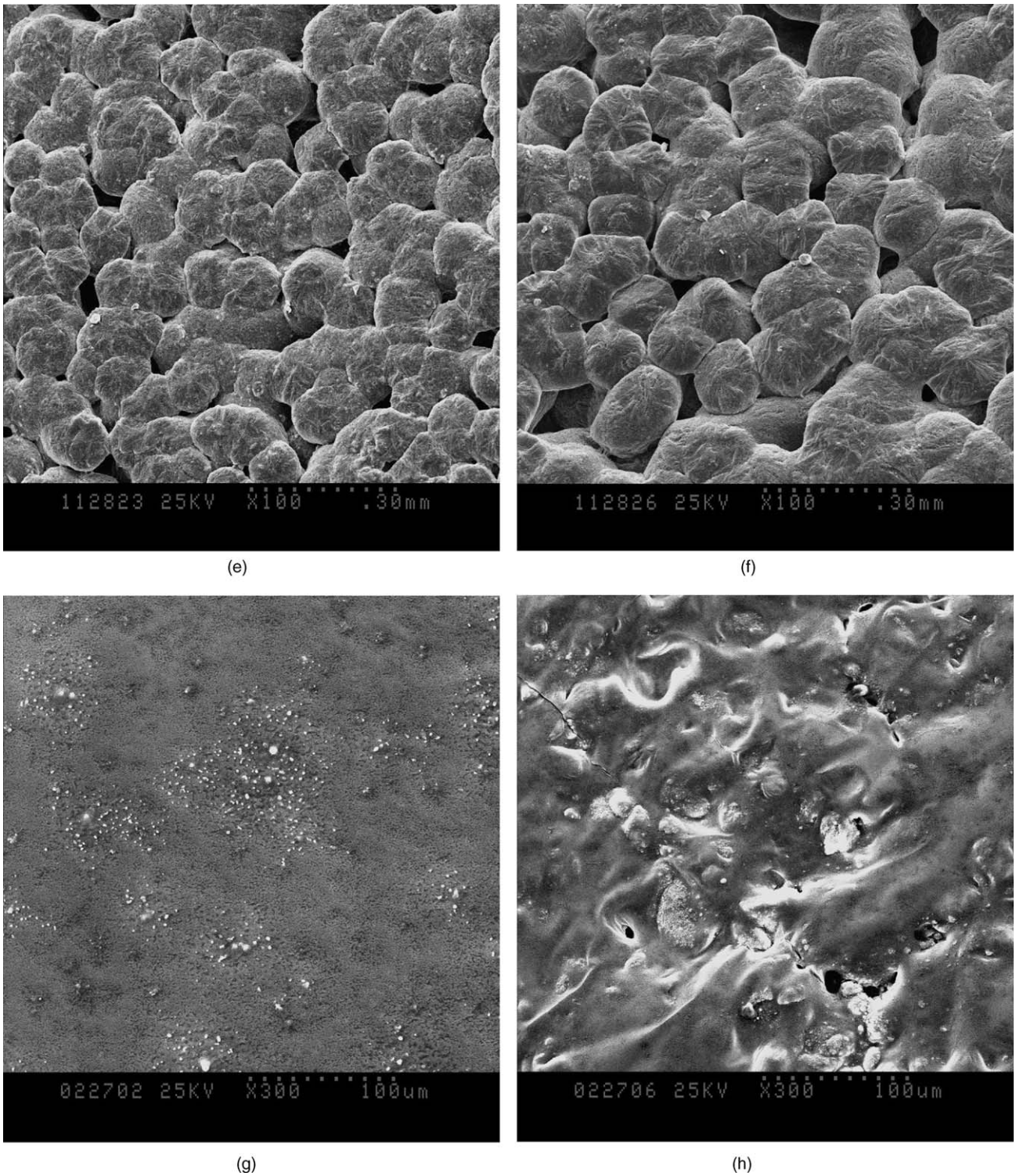


(e) (f)

(g) (h)

Fig. 6. (*Continued*)

exhibit a steady decline even while their widths increase. On the other hand, the intensity of other peaks at 1642.9, 2856.06, 2924.9 and 3441.7 $cm^{-1}$ in $Li_{1.3}Al_{0.3}Ti_{1.7}(PO_4)_3$ increases, even while their widths increase, with decreasing $Li_{1.3}Al_{0.3}Ti_{1.7}(PO_4)_3$ content. When this content is 15 or 20 wt.%, a new peak, located in a similar position to that for EO/Li = 8, 12 and 16, clearly appeared (Fig. 5(B)). Additionally, peaks at 632.54, 1095.37, 1639.19, 2013.32 and 3438.46 $cm^{-1}$ in $LiClO_4$ also merged at a corresponding location in the PEO–$LiClO_4$–$Li_{1.3}Al_{0.3}Ti_{1.7}(PO_4)_3$ films over the range of $Li_{1.3}Al_{0.3}Ti_{1.7}(PO_4)_3$ content from 10 to 40 wt.%. Nevertheless, the peaks at 632.54 and 1095.37 $cm^{-1}$ in $LiClO_4$ do not distinctly appear in 5 wt.% $Li_{1.3}Al_{0.3}Ti_{1.7}(PO_4)_3$, which has the highest $LiClO_4$ content

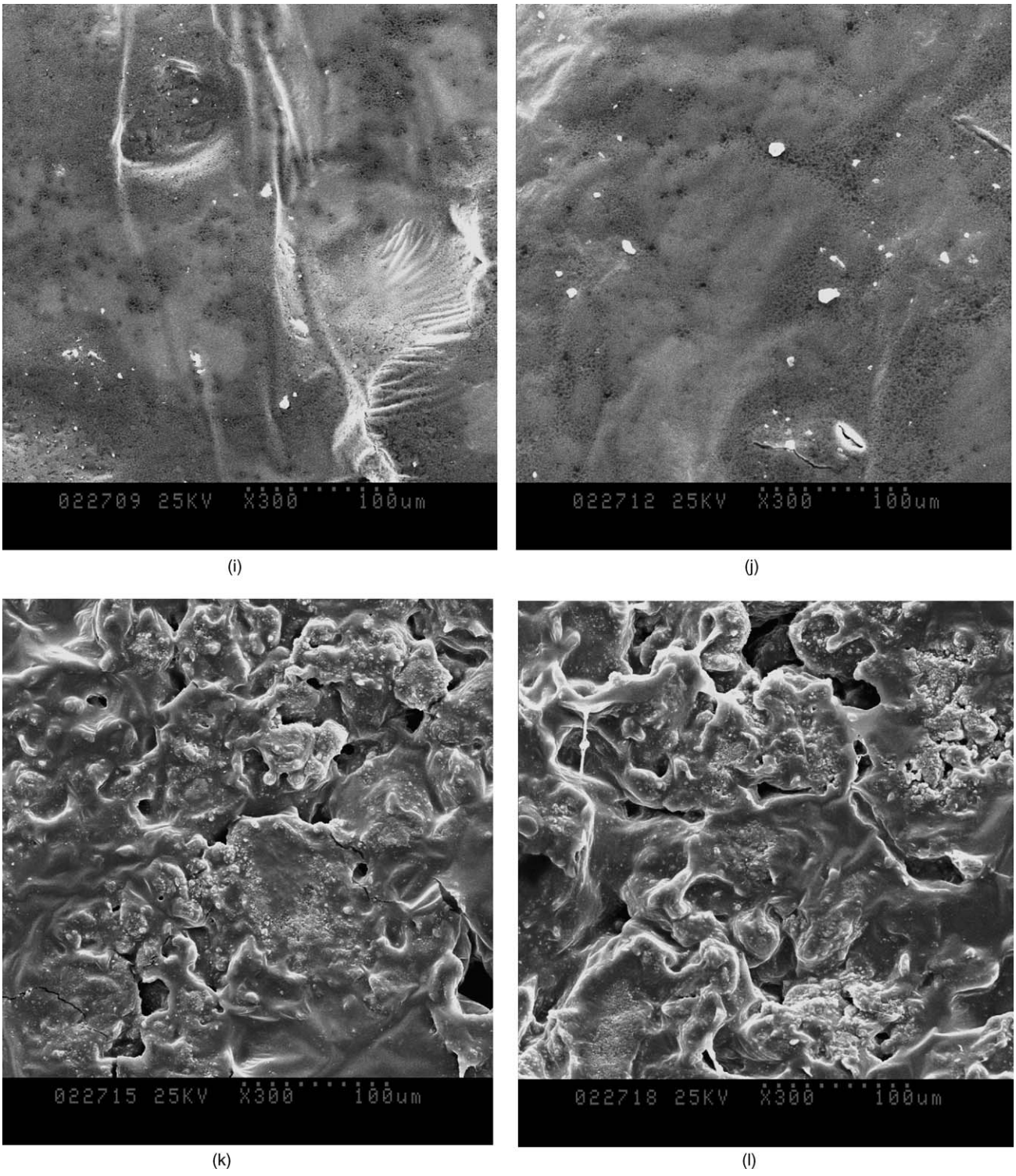


Fig. 6. (*Continued*)

among all PEO–$LiClO_4$–$Li_{1.3}Al_{0.3}Ti_{1.7}(PO_4)_3$ samples. This result possibly indicates that $LiClO_4$ forms a complexation with PEO, despite the absence of any similar results for the changes of other peaks.

Therefore, as demonstrated by all of the above results, the changes in the PEO–$Li_{1.3}Al_{0.3}Ti_{1.7}(PO_4)_3$ and PEO–$LiClO_4$–$Li_{1.3}Al_{0.3}Ti_{1.7}(PO_4)_3$ films that are evident in Fig. 5 directly support complexation between $LiClO_4$ and PEO and a finite complexation between $Li_{1.3}Al_{0.3}Ti_{1.7}(PO_4)_3$ and PEO. Furthermore, the latter complexation depends on the $Li_{1.3}Al_{0.3}Ti_{1.7}(PO_4)_3$ content in PEO.

### 3.4. SEM studies

The surface morphologies of PEO–$Li_{1.3}Al_{0.3}Ti_{1.7}(PO_4)_3$ films with different EO/Li ratios, PEO–$LiClO_4$–$Li_{1.3}Al_{0.3}Ti_{1.7}$

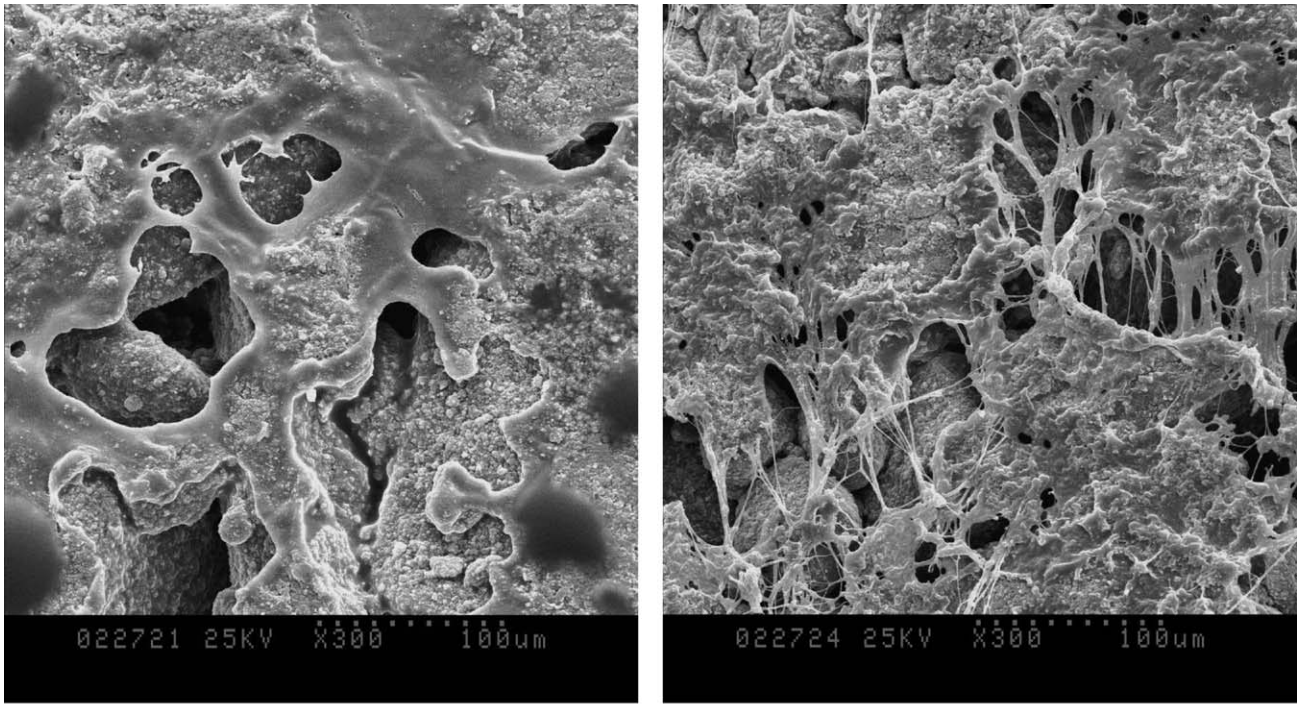


(m) (n)

Fig. 6. (*Continued*).

$(PO_4)_3$ films with different $Li_{1.3}Al_{0.3}Ti_{1.7}(PO_4)_3$ content, pure PEO film and fine $Li_{1.3}Al_{0.3}Ti_{1.7}(PO_4)_3$ powders are shown in Fig. 6.

Some larger spherulites and other amorphous regions between spherulites are observed in pure PEO. The addition of $Li_{1.3}Al_{0.3}Ti_{1.7}(PO_4)_3$, whose particle size in Fig. 6 is consistent with that in Fig. 1, changes the morphology of the film surface. Instead of a spherulite-type structure, cell-type microstructures in PEO–$Li_{1.3}Al_{0.3}Ti_{1.7}(PO_4)_3$ films are observed and the average cell size is reduced with decreased EO/Li molar ratio until EO/Li = 12. At EO/Li = 8, the cell structure becomes irregular, probably because the high $Li_{1.3}Al_{0.3}Ti_{1.7}(PO_4)_3$ content cannot be well dissolved in PEO, and thereby roughen the cell surface. The cells in the PEO–$Li_{1.3}Al_{0.3}Ti_{1.7}(PO_4)_3$ films with different EO/Li molar ratios are, however, much smaller than the spherulites in pure PEO. The formation of the smooth and regular cellular structure may be attributed to complexation of PEO with $Li_{1.3}Al_{0.3}Ti_{1.7}(PO_4)_3$ to some extent. After PEO is introduced into acetonitrile, the PEO dissolves and the PEO spherulites collapsed into small crystallites that are randomly dispersed but flexibly interconnected by amorphous chain segments in the acetonitrile solvent.

After the acetonitrile is evaporated, the complexation between the $Li_{1.3}Al_{0.3}Ti_{1.7}(PO_4)_3$ particles suspended in the solvent and the amorphous chains in PEO piled on to the crystallites to form a cell. Each cell may contain a crystallite at the center that is surrounded by a covering of the complexed part. The cells contact each other to facilitate lithium-ion conduction. Some pores are seen in the micrographs and may have been caused by non-controllable evaporation of the acetonitrile.

With the addition of $Li_{1.3}Al_{0.3}Ti_{1.7}(PO_4)_3$ and $LiClO_4$ to the PEO–$LiClO_4$–$Li_{1.3}Al_{0.3}Ti_{1.7}(PO_4)_3$ films over a $Li_{1.3}Al_{0.3}Ti_{1.7}(PO_4)_3$ content range from 5 to 40 wt.%, the surface morphology of PEO is changed severely. Some PEO spherulites in the PEO–$LiClO_4$–$Li_{1.3}Al_{0.3}Ti_{1.7}(PO_4)_3$ films are almost destroyed in contrast to those in pure PEO and PEO–$Li_{1.3}Al_{0.3}Ti_{1.7}(PO_4)_3$ films with different EO/Li molar ratios. As the $Li_{1.3}Al_{0.3}Ti_{1.7}(PO_4)_3$ content is decreased from 40 to 5%, although the $LiClO_4$ content increases, the surface morphology undergoes a dramatic improvement from rough to smooth. The smooth morphology is closely related to the reduction of PEO crystallinity in the presence of $LiClO_4$ and $Li_{1.3}Al_{0.3}Ti_{1.7}(PO_4)_3$. These results are in good agreement with the decreased degree of crystallinity that is found from the DSC measurements, see Table 1. These changes also indicate that the addition of $LiClO_4$ imparts far more damage to the PEO spherulites than does $Li_{1.3}Al_{0.3}Ti_{1.7}(PO_4)_3$, although the latter changes the size of the PEO spherulites, which is important for high ionic conductivity.

### 3.5. Conductivity measurements

The ionic conductivity of different samples was also measured as a function of temperature. Typical variations in the ionic conductivity of $Li_{3-2x}(Al_{1-x}Ti_x)_2(PO_4)_3$ ($x = 0.55$–$1.0$) with change in temperature using Pt blocking electrodes are shown in Fig. 7(A). Any slight change in slope, which mimics a phase transition, is measured. In the $Li_{3-2x}(Al_{1-x}Ti_x)_2(PO_4)_3$ system, the compound $Li_{1.3}Al_{0.3}Ti_{1.7}(PO_4)_3$ with $x = 0.85$ exhibits the highest conductivity over almost the whole temperature range, i.e. $9.210 \times 10^{-4}$ S cm$^{-1}$ at 613 K and $1.792 \times 10^{-6}$ S cm$^{-1}$ at

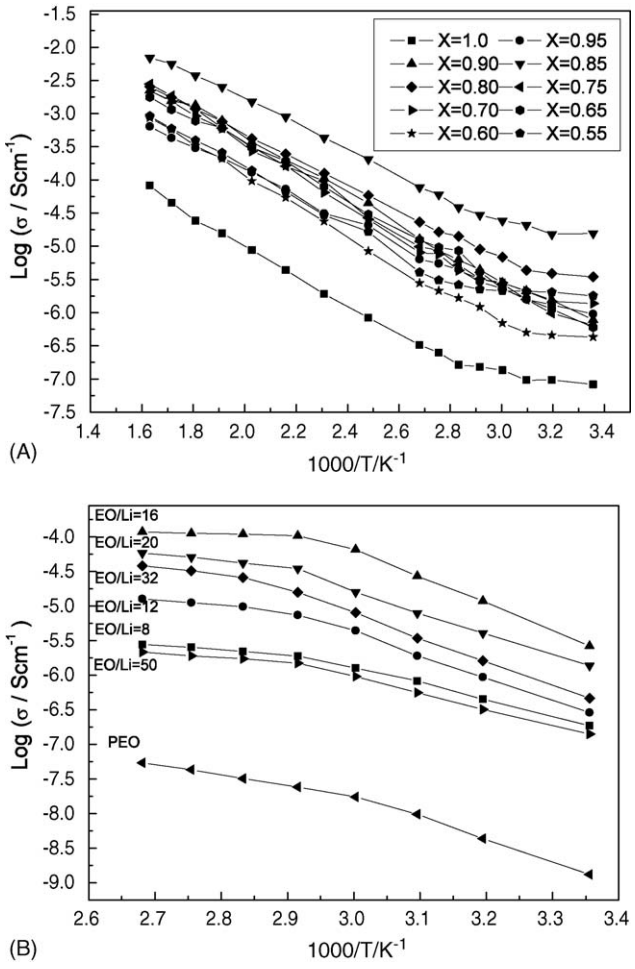


Fig. 7. (A) Temperature dependence of ionic conductivity of $Li_{3-2x}(Al_{1-x}Ti_x)_2(PO_4)_3$. (B) Temperature dependence of ionic conductivity of PEO–$Li_{1.3}Al_{0.3}Ti_{1.7}(PO_4)_3$ with various EO/Li molar ratios (in addition to PEO's conductivity).

room temperature. The temperature dependence of the ionic conductivity PEO–$Li_{1.3}Al_{0.3}Ti_{1.7}(PO_4)_3$ films with different EO/Li molar ratios is plotted in Fig. 7(B). In each plot, there are two linear trends below and above $T_c$, which suggests an Arrhenius-type thermally-activated process. This is in good agreement with the DSC results that show a progressive shift of the main melting peak with decreasing salt concentration (see Fig. 4(A)). It is concluded that the $T_c$ of the PEO matrix divides the conductivity curve for each specimen, into two parts, corresponding to two Arrhenius relations with two different activation energies. The conductivity, $\sigma$, can be expressed as:

$$\sigma = \sigma_0 \exp\left(\frac{-E_a}{KT}\right) \quad (1)$$

where $\sigma_0$ is a pre-exponential factor, $E_a$ the activation energy, and $K$ the Boltzmann constant. The calculated activation energies ($E_a$) for PEO–$Li_{1.3}Al_{0.3}Ti_{1.7}(PO_4)_3$ are given in Table 2.

The conductivity increases with increasing temperature for all compositions of the PEO–$Li_{1.3}Al_{0.3}Ti_{1.7}(PO_4)_3$ system with different EO/Li molar ratios, see Fig. 7(B). This behaviour can be explained in terms of a hopping mechanism between coordinating sites, local structural relaxations and segmental

Table 2
Activation energies of PEO–$Li_{1.3}Al_{0.3}Ti_{1.7}(PO_4)_3$ with different EO/Li molar ratios

| EO/Li molar ratio | $E_a$ (above $T_m$) (eV) | $E_a$ (below $T_m$) (eV) |
|---|---|---|
| Pure PEO | 2.988 | 6.393 |
| EO/Li = 50 | 1.336 | 4.687 |
| EO/Li = 32 | 3.184 | 6.907 |
| EO/Li = 20 | 1.929 | 5.961 |
| EO/Li = 16 | 0.475 | 7.823 |
| EO/Li = 12 | 1.924 | 6.603 |
| EO/Li = 8 | 1.446 | 4.766 |

motions of polymer. At temperatures above $T_m$, the polymer chain becomes more flexible with the progressively increasing amorphous region so that the bond rotations produce segmental motion. This structural change favours hopping inter- and intra-chain ion movements so that the conductivity of the polymer electrolyte becomes higher. At any temperature in Fig. 7(C), the maximum conductivity occurs at EO/Li = 16. The lithium ion conductivity depends on not only the concentration, but also on the mobility of the lithium ions. An EO/Li ratio of 16 manifests the best trade-off between ion concentration and ion mobility, and therefore gives the best ionic conductivity. Moreover, the addition of $Li_{1.3}Al_{0.3}Ti_{1.7}(PO_4)_3$ to the PEO polymer matrix as the EO/Li molar ratio is decreased from 50 to 8 not only increases the number of free ions and available sites for free ions in the polymer matrix [19], but also improves the plasticity of the polymer. Both these characteristics promote ion conduction. Nevertheless, the conductivity decreases as the EO/Li molar ratio is decreased further from 16 to 8 with further increases in $Li_{1.3}Al_{0.3}Ti_{1.7}(PO_4)_3$ content. This may result from the plasticizing effect of the salt being weakened by too much salt, i.e. the plasticizing effect of the salt is maximum at an EO/Li molar ratio of 16. With increase in $Li_{1.3}Al_{0.3}Ti_{1.7}(PO_4)_3$ salt content, the probability of ion-pair [20,21] formation is enhanced and the number of available sites for the free ions is limited in the polymer electrolyte. This reduces the mean free path of the free ions and, therefore, also the conductivity. The ionic conductivities of the PEO–$Li_{1.3}Al_{0.3}Ti_{1.7}(PO_4)_3$ polymer electrolytes with EO/Li molar ratios ranging from 8 to 50 are all higher than $10^{-7}$ S cm$^{-1}$ at room temperature, and the highest conductivities (e.g. $1.185 \times 10^{-4}$ S cm$^{-1}$ at 373 K and $2.631 \times 10^{-6}$ S cm$^{-1}$ at room temperature) are obtained when the EO/Li molar ratio is 16. The ionic conducting behaviour of the PEO–$Li_{1.3}Al_{0.3}Ti_{1.7}(PO_4)_3$ polymer electrolyte demonstrates that it can be used as the solid electrolyte for lithium batteries at medium and high temperatures.

The ionic conductivity of the PEO–$LiClO_4$–$Li_{1.3}Al_{0.3}Ti_{1.7}(PO_4)_3$ film with EO/Li = 8 as a function of temperature is given in Fig. 8(A). The curve shows a deviation from Arrhenius behaviour, that can be described by the empirical Vogel–Tammann–Fulcher (VTF) expression (Eq. (2)) and that may be related to free volume-based theories of mobility, i.e.

$$\sigma = AT^{-1/2} \exp\left[\frac{-B}{K_B(T - T_0)}\right] \quad (2)$$

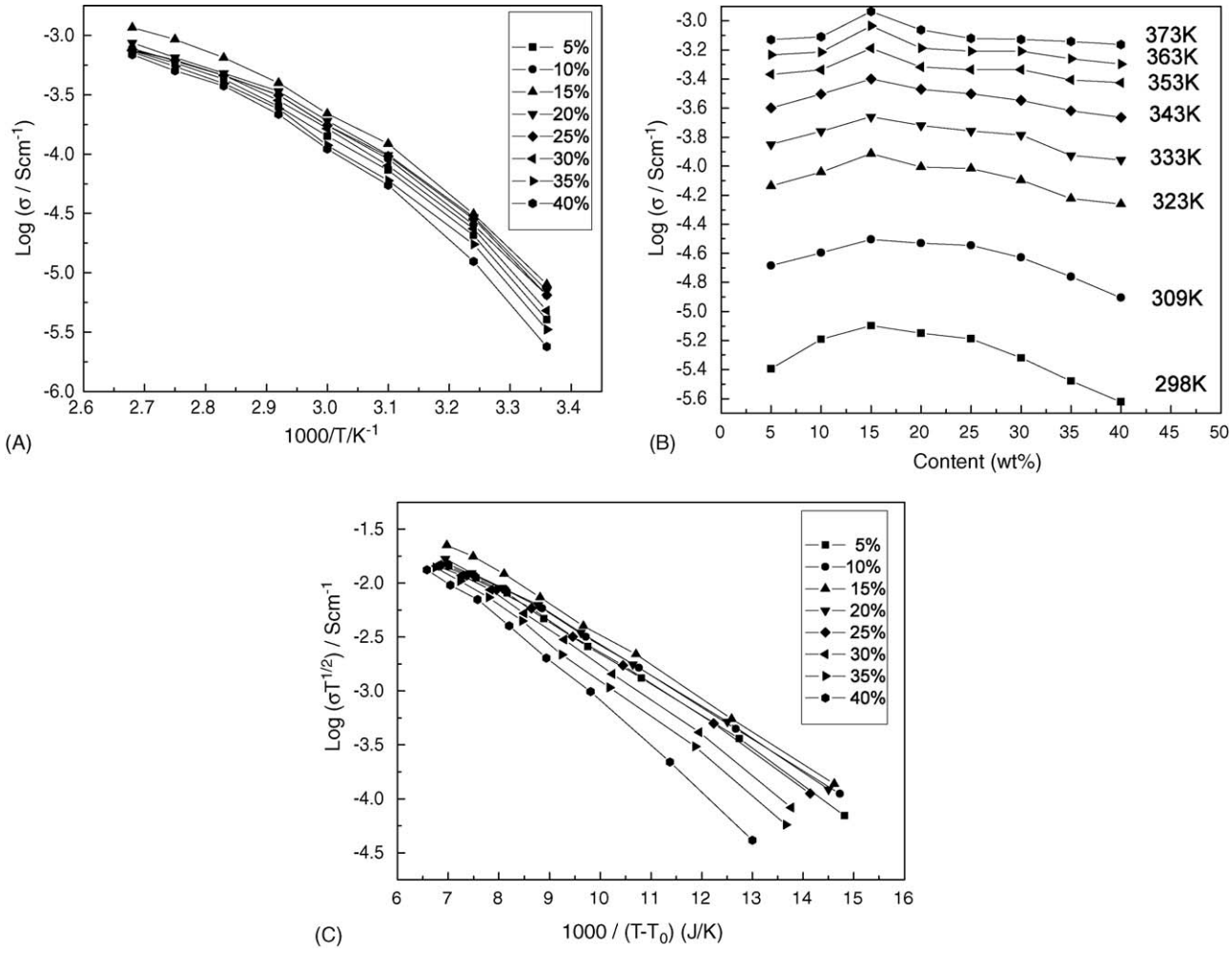


Fig. 8. (A) Temperature dependence of conductivity of PEO–$LiClO_4$–$Li_{1.3}Al_{0.3}Ti_{1.7}(PO_4)_3$ composite polymer electrolytes at different $Li_{1.3}Al_{0.3}Ti_{1.7}(PO_4)_3$ contents. (B) Ionic conductivities as function of $Li_{1.3}Al_{0.3}Ti_{1.7}(PO_4)_3$ content for PEO–$LiClO_4$–$Li_{1.3}Al_{0.3}Ti_{1.7}(PO_4)_3$ composite polymer electrolytes at various temperatures. (C) VTF plots of $\log(\sigma T^{1/2})$ vs. reciprocal $(T - T_0)$ for the system PEO–$LiClO_4$–$Li_{1.3}Al_{0.3}Ti_{1.7}(PO_4)_3$ system at different $Li_{1.3}Al_{0.3}Ti_{1.7}(PO_4)_3$ contents.

where $A$ is a pre-exponential factor; $B$ a pseudoactivation energy for conduction; $K$ the Boltzmann constant; $T_0$ a thermodynamic $T_g$, that is usually 30–50 K lower than $T_g$ calculated from DSC experiments [22,23]. Based on this model, the VTF plots of $\log(\sigma T^{1/2})$ versus $1/(T - T_0)$ for PEO–$LiClO_4$–$Li_{1.3}Al_{0.3}Ti_{1.7}(PO_4)_3$ films with $Li_{1.3}Al_{0.3}Ti_{1.7}(PO_4)_3$ contents ranging from 5 to 40 wt.% are plotted in Fig. 8(C). The approximately straight lines clearly confirm that the temperature dependence of conductivity obeys the VTF relationship.

The ionic conductivity of the PEO–$LiClO_4$–$Li_{1.3}Al_{0.3}Ti_{1.7}(PO_4)_3$ CPE with EO/Li = 8 as a function of content at various temperatures (Fig. 8(B)) clearly show that the ionic conductivity increases with increasing $Li_{1.3}Al_{0.3}Ti_{1.7}(PO_4)_3$ content until the maximum conductivities are reached at a content of 15 wt.% (i.e. $1.161 \times 10^{-3}$ S cm$^{-1}$ at 373 K and $7.985 \times 10^{-6}$ S cm$^{-1}$ at room temperature). Thereafter, the conductivity decreases. In general, it is possibly true that the ion mobility, the number of free ions and the volume fraction of the amorphous phase in a polymer electrolyte are important factors for enhancing its ionic conductivity. The ion mobility and ion number are intrinsically determined by the lithium salt and the complexation between the salt and the polymer matrix. With the addition of extra, non-conducting, ceramic fillers such as $SiO_2$, $TiO_2$, $Al_2O_3$ and SiC the enhanced conductivity reaches $10^{-4}$ S cm$^{-1}$ at 373 K (i.e. at above the melting point), while remaining at $10^{-6}$ to $10^{-7}$ S cm$^{-1}$ at room temperature [8,9]. Such values are all much lower than the equivalent values obtained in this study for the PEO–$LiClO_4$–$Li_{1.3}Al_{0.3}Ti_{1.7}(PO_4)_3$ films. Thus, the present findings confirm the advantage of $Li_{1.3}Al_{0.3}Ti_{1.7}(PO_4)_3$ as a filler, not only by producing a stronger reduction of crystallinity and more flexible local chains in the amorphous phase as indicated by the lower $T_g$ (see Fig. 4(B) and Table 1), but also by possible dissolution and complexation with PEO. When, however, the $Li_{1.3}Al_{0.3}Ti_{1.7}(PO_4)_3$ content is raised above 15 wt.% the CPE crystallinity is increased (Table 1), which reduces the volume fraction of the amorphous phase, stiffens the molecular chain and decreases the flexibility of the chain. These changes occur despite the continued decrease in $T_g$ with the increase in $Li_{1.3}Al_{0.3}Ti_{1.7}(PO_4)_3$ content, as shown by DSC curves. This

indicates a decreased number and retarded transfer of free ions in PEO. In addition, these is a greatest probability of ion-pair [19] formation in the PEO–$LiClO_4$–$Li_{1.3}Al_{0.3}Ti_{1.7}(PO_4)_3$ system that, in turn, decreases both the number of free ions and the ion mobility. As a result, the ionic conductivity decreases. According to the observed data, however, the conductivities of the PEO–$LiClO_4$–$Li_{1.3}Al_{0.3}Ti_{1.7}(PO_4)_3$ films are higher than those of the PEO–$Li_{1.3}Al_{0.3}Ti_{1.7}(PO_4)_3$ films at all temperatures.

## 4. Conclusions

For the use of $Li_{1.3}Al_{0.3}Ti_{1.7}(PO_4)_3$ as a lithium fast ionic conductor to produce the best ionic conductivity in $Li_{3-2x}(Al_{1-x}Ti_x)_2(PO_4)_3$ ($x = 0.55$–$1.0$), $Li_{1.3}Al_{0.3}Ti_{1.7}(PO_4)_3$-filled, PEO-based, CPE films are prepared by means of a solution-cast technique. X-ray diffraction analyses of the as-prepared films reveal that: (i) $Li_{1.3}Al_{0.3}Ti_{1.7}(PO_4)_3$ has a strong effect on the crystallization of the PEO matrix and complexes with PEO to some extent; (ii) $LiClO_4$, which decreases the crystallization of the polymer electrolyte, complexes more easily with PEO than $Li_{1.3}Al_{0.3}Ti_{1.7}(PO_4)_3$. Differential scanning calorimetry experiments show that the $T_m$ of the PEO matrix in PEO–$Li_{1.3}Al_{0.3}Ti_{1.7}(PO_4)_3$ films is lowered with increasing the $Li_{1.3}Al_{0.3}Ti_{1.7}(PO_4)_3$ content, and that the $T_g$ of the PEO–$LiClO_4$–$Li_{1.3}Al_{0.3}Ti_{1.7}(PO_4)_3$ films decreases and although $T_m$ and $\chi_c$ increase as the $Li_{1.3}Al_{0.3}Ti_{1.7}(PO_4)_3$ content is increased despite the fact that $LiClO_4$ is decreased. These results combine to indicate that the crystallinity of the PEO matrix deteriorates, which is an advantageous step in improving the ionic conductivity of PEO.

In contrast with IR absorption spectra for the PEO–$Li_{1.3}Al_{0.3}Ti_{1.7}(PO_4)_3$ films, it is clear that $LiClO_4$ in PEO–$LiClO_4$–$Li_{1.3}Al_{0.3}Ti_{1.7}(PO_4)_3$ films complexes more easily with PEO than does $Li_{1.3}Al_{0.3}Ti_{1.7}(PO_4)_3$. Analysis of the IR absorption spectra for $Li_{1.3}Al_{0.3}Ti_{1.7}(PO_4)_3$-filled, PEO-based CPEs in this study confirms that the complexation between $Li_{1.3}Al_{0.3}Ti_{1.7}(PO_4)_3$ and PEO depends strongly on the $Li_{1.3}Al_{0.3}Ti_{1.7}(PO_4)_3$ content.

Scanning electron micrographs indicate some severe changes in the surface morphologies of the $Li_{1.3}Al_{0.3}Ti_{1.7}(PO_4)_3$-filled, PEO-based CPEs. The addition of $Li_{1.3}Al_{0.3}Ti_{1.7}(PO_4)_3$ decreases the size of the PEO spherulites. The ionic conductivity of the PEO-based, CPE films is found to be strongly related to both temperature and $Li_{1.3}Al_{0.3}Ti_{1.7}(PO_4)_3$ content. For CPE films made from PEO and $Li_{1.3}Al_{0.3}Ti_{1.7}(PO_4)_3$, the ionic conductivities are maximized at $1.185 \times 10^{-4}$ S cm$^{-1}$ at 373 K and $2.631 \times 10^{-6}$ S cm$^{-1}$ at room temperature, at an EO/Li molar ratio of 16. The temperature dependence of the ionic conductivity the PEO–$LiClO_4$–$Li_{1.3}Al_{0.3}Ti_{1.7}(PO_4)_3$ films follow the empirical Vogel–Tammann–Fulcher (VTF) expression rather than the classical Arrhenius law. With $Li_{1.3}Al_{0.3}Ti_{1.7}(PO_4)_3$ acting as both a filler and an ion conductor, the ionic conductivities of the PEO–$LiClO_4$–$Li_{1.3}Al_{0.3}Ti_{1.7}(PO_4)_3$ films are maximized at $1.161 \times 10^{-3}$ S cm$^{-1}$ at 373 K and $7.985 \times 10^{-6}$ S cm$^{-1}$ at room temperature, at a $Li_{1.3}Al_{0.3}Ti_{1.7}(PO_4)_3$ content of 15 wt.%.

## Acknowledgement

This work was sponsored by Korea Research Foundation (Grant #KRF-2004-05-D00064).

## References

[1] P.V. Wright, Br. Polym. J. 7 (1975) 319.
[2] M.B. Armand, J.M. Chabagno, M. Duclot, in: Extended Abstracts of the Second International Symposium on Solid Electrolytes, St. Andrews, Scotland, 1978.
[3] M.B. Armand, J.M. Chabagno, M. Duclot, in: P. Vashishta, J.N. Mundy, G.D. Shennoy (Eds.), Fast Ion Transport in Solids, North-Holland, New York, 1979.
[4] Z. Gadjourova, Y.G. Andreev, D.P. Tunstall, P.G. Bruce, Nature 412 (2001) 520.
[5] C.C. Tambelli, A.C. Bloise, A.V. Rosario, E.C. Pereira, C.J. Magon, J.P. Donoso, Electrochim. Acta 47 (2002) 1677.
[6] C. Capiglia, P. Mustarelli, E. Quartarone, C. Tomasi, A. Magistris, Solid State Ion. 118 (1999) 73.
[7] P.P. Chu, M. Jaipal Reddy, J. Power Sources 115 (2003) 288.
[8] F. Croce, G.B. Appetecchi, L. Persi, B. Scrosati, Nature 394 (1998) 456.
[9] B.K. Choi, Y.W. Kim, K.H. Shin, J. Power Sources 68 (1997) 357.
[10] T. Suzuki, K. Yoshida, K. Uematsu, T. Kodama, K. Toda, Z.-G. Ye, M. Ohashi, M. Sato, Solid State Ion. 113–115 (1998) 89.
[11] A.B. Bykov, A.P. Chirkin, L.N. Demyanets, S.N. Doronin, E.A. Genkina, A.K. Ivanov-Shits, I.P. Kondratyuk, B.A. Maksimov, O.K. Mel'Nikov, L.N. Muradyan, V.I. Simonov, V.A. Timofeeva, Solid State Ion. 38 (1990) 31.
[12] H. Aono, E. Sugimoto, Y. Sadaoka, N. Imanaka, G. Adachi, J. Electrochem. Soc. 137 (1990) 1023.
[13] K. Ado, Y. Saito, T. Asai, H. Kageyama, O. Nakamura, Solid State Ion. 53–56 (1992) 723.
[14] Y. Saito, K. Ado, T. Asai, H. Kageyama, O. Nakamura, J. Mater. Sci. Lett. 11 (1992) 888.
[15] T. Suzuki, K. Yoshida, K. Uematsu, T. Kodama, K. Toda, Z.-G. Ye, M. Sato, Solid State Ion. 104 (1997) 27.
[16] Y.G. Andreev, P.G. Bruce, Electrochim. Acta 45 (2000) 1417.
[17] S.J. Wen, T.J. Richardson, D.I. Ghantous, K.A. Striebel, P.N. Ross, E.J. Cairns, J. Electroanal. Chem. 408 (1996) 113.
[18] C.P. Rhodes, R. Frech, Solid State Ion. 136–137 (2000) 1131.
[19] C. Julien, G.-A. Nazri, Solid State Batteries: Materials Design and Optimization, Kluwer Academic Publishers, USA, 1994.
[20] F.M. Gray, Polymer Electrolytes, Royal Society of Chemistry Monographs, Cambridge, 1997.
[21] G.B. Appetecchi, W. Henderson, P. Villano, M. Berrettoni, S. Passerini, J. Electrochem. Soc. 148 (10) (2001) A1171.
[22] M. Siekierski, W. Wieczorek, J. Przyluski, Electrochim. Acta 43 (1997) 1339.
[23] V. Munchow, V. Di Noto, E. Tondello, Electrochim. Acta 45 (2000) 1211.